JOURNAL OF MATERIALS SCIENCE 14 (1979) 2353–2365

Urania–yttria solid solution electrodes for high-temperature electrochemical applications

S. P. S. BADWAL, D. J. M. BEVAN
School of Physical Sciences, The Flinders University of South Australia, Bedford Park, Adelaide, Australia 5042

Measurements of total electrical conductivity on fluorite-type U_3O_8–Y_2O_3 (Sc_2O_3) solid solutions have been made as a function of temperature and U/Y(Sc) ratio. The following compositions were studied: $(U_{0.7}Y_{0.3})O_{2+x}$, $(U_{0.6}Y_{0.4})O_{2+x}$, $(U_{0.5}Y_{0.5})O_{2+x}$, $(U_{0.45}Y_{0.55})O_{2+x}$, $(U_{0.4}Y_{0.6})O_{2+x}$, $(U_{0.35}Y_{0.65})O_{2+x}$, $(U_{0.3}Y_{0.7})O_{2-x}$, $(U_{0.5}Sc_{0.5})O_{2+x}$ and $(U_{0.38}Sc_{0.62})O_{2+x}$. Preliminary measurements on the latter two compositions were carried out for comparison purposes. The maximum conductivity value occurred for the U_3O_8–Sc_2O_3 solid solutions, and for $(U_{0.7}Y_{0.3})O_{2+x}$ in the U_3O_8–Y_2O_3 system. The conductivity in these fluorite-type solid solutions is mainly electronic, the conduction mechanism being hopping-type. The energy of activation lay between 25 and 40 kJ mol^{-1}. The $(U_{0.3}Y_{0.7})O_{2-x}$ composition appeared to be an ionic conductor with an activation energy of $\sim$ 110 kJ mol^{-1} below 800 to 850° C. The diffusion of cations of U_3O_8–Y_2O_3 into ZrO_2–Y_2O_3 was studied during passage of current: no observable diffusion occurred over the period of current passage (384 h). Attempts were made to determine the anionic contribution to the total conductivity in U_3O_8–Y_2O_3 solid solutions using the blocking electrode technique. Results indicated that complete isolation of the specimen–blocking electrode (YSZ) interface from the ambient gases is necessary if such measurements are to be reliable. The diffusion coefficients calculated from the conductivity data using the Nernst–Einstein relation were two orders of magnitude higher than those obtained by a direct method.

1. Introduction

Both decreasing fossil fuel resources and concern over thermal and chemical pollution have led in the last ten years to increased interest in high-temperature fuel cells [1–6] and high-temperature electrolysis of steam [7,8]. In the former, electrical energy can be generated by the direct electrochemical conversion of the chemical energy of the fuel and oxidant: by reversing the mode of operation of a high-temperature solid electrolyte fuel cell, electrolysis of steam can be achieved to produce hydrogen for conventional usage.

Although there are advantages in the high-temperature (800 to 1100° C) of operation compared to low-temperature operation of fuel cells and steam electrolysers in terms of waste heat usage and in terms of the fast electode kinetics expected, many material problems arise when it comes to the choice of electrodes and electrolyte.

The solid oxide electrolytes with fluorite-type structure are ideally suited for fuel cell applications, since current in them is carried by oxide ions, and oxygen is the universally available oxidant. The conductivity of these solid oxides is, however, low at lower temperatures, and they can be used only in the temperature range 800 to 1200° C where the conductivity reaches practicable values. At a nominal cell operating temperature of 1000° C, the best conductivity is exhibited by calcia and rare-earth stabilized zirconias [9–13], scandia stabilized zirconia having the maximum conductivity ($\simeq 0.21\,\Omega^{-1}\,cm^{-1}$). The anionic transport number is close to one in these electrolytes for both oxidizing and reducing

0022–2461/79/102353–13 $03.30/0

atmospheres at 1000° C. Other electrolyte materials which have been studied include $CeO_2-Y_2O_3$, CeO_2-CaO, $CeO_2-La_2O_3$, $HfO_2-Y_2O_3$ and $ThO_2-Y_2O_3$ [13–17]. However in these systems the range of oxygen pressure over which the anionic transport number is unity is narrower than in the case of calcia or rare-earth stabilized zirconia. Yttria stabilized zirconia appears to be the best available electrolyte at present.

A potential electrode material is assessed according to the following criteria, which will be governed by the environment of the electrode: the electrode must have high electronic conductivity (20 to 50 Ω^{-1} cm^{-1}), a very low vapour pressure at operating temperature, and must be chemically inert. Ideally, its thermal expansion should match that of the electrolyte used, and there should be minimum irreversible energy losses.

Various metal oxides and metals have been studied as electrodes [10, 18–23]. So far only noble metals partially fulfil the above requirements. Among other materials studied, cobalt, nickel and iron seem to be suitable anode materials, while for the cathode Sn-doped In_2O_3, some perovskite-type mixed oxides and copper maganite have been explored. Most of these materials suffer from one defect or another.

Based on the philosophy that the electrode material most likely to be compatible with the fluorite-type electrolyte is itself fluorite-type, the main emphasis in this study has been on such materials. Urania and the rare-earths (including yttria and scandia) for solid solutions in air or oxygen which have the fluorite-type structure over a wide composition range (e.g., 30 to 70 mol % $YO_{1.5}$ [24, 25]), and these are structurally stable in strongly reducing atmospheres such as CO or hydrogen. All that reduction does is to change the average oxidation state of uranium and the overall oxygen–metal ratio.

This paper thus reports the results of detailed studies of these materials from the point of view of their suitability as high-temperature oxide electrodes. It includes data on total conductivity, transport numbers and interdiffusion of the electrode and electrolyte cations. The other major aspect of electrode processes is discussed elsewhere [26].

2. Experimental

2.1. Preparation and characterization of materials

U_3O_8, Y_2O_3, Cu and Cu_2O were purchased from Koch-Light Laboratories Limited and were 99.97% pure.

CeO_2 was purchased from Johnson Matthey Chemicals Limited as spectroscopically pure material.

Sc_2O_3 was prepared from the chloride solution [27] by homogeneous precipitation of the oxalate with dimethyloxalate. This was subsequently ignited in air to form the oxide.

To prepare solid solutions of $U_3O_8-Y_2O_3$ and $U_3O_8-Sc_2O_3$, a nitric acid solution of U_3O_8 and $Y(Sc)_2O_3$ containing the desired amounts was prepared, and the hydroxide co-precipitated by addition of excess ammonia solution. The precipitate was washed, dried and decomposed at 900° C in air, ground in an agate mortar and pressed into

TABLE I Preparation details

Sample	Reaction temperature (± 10° C)* and time (h)	Sintering temperature (± 10° C)* and time (h) for pellets
$(U_{0.7}Y_{0.3})O_{2+x}$†	1465 (100)	1410 (100)
$(U_{0.6}Y_{0.4})O_{2+x}$	1350 (90)	1385 (100)
$(U_{0.5}Y_{0.5})O_{2+x}$	1200 (72)	1350 (100)
$(U_{0.45}Y_{0.55})O_{2+x}$	1260 (50)	1390 (100)
$(U_{0.4}O_{0.6})O_{2+x}$	1200 (72)	1385 (100)
$(U_{0.35}Y_{0.65})O_{2+x}$	1260 (50)	1375 (100)
$(U_{0.3}Y_{0.7})O_{2-x}$	975 (35)	1380 (100)
$(U_{0.7}Y_{0.3})O_{2+x}$ (argon)	1470 (100)	1520 (100)
$(U_{0.5}Sc_{0.5})O_{2+x}$	1350 (100)	1400 (100)
$(U_{0.38}Sc_{0.62})O_{2+x}$	1350 (100)	1400 (100)

*Firing was carried in air unless otherwise specified.
†Loss of weight observed.

pellets of 12.5 mm diameter. These pellets were then heated in air (unless otherwise specified) to higher temperatures ranging from 1200 to 1500° C in a molybdenum-wound furnace to complete the reaction. Table I summarizes the preparation of all samples studied.

Sintered discs of ZrO_2–10 mol% Y_2O_3, used as electrolyte, were purchased from Ceramic Oxide Fabricators Pty. Ltd., Australia. These had a density about 88% of theoretical.

All specimens were characterized and checked for complete reaction by X-ray powder diffraction: measured parameters were in agreement with those already reported [24, 28, 29].

Urania–yttria (scandia) pellets, as prepared, were ground to less than 50 μm diameter, the powder pressed again into discs of 12.5 or 15.6 mm diameter at a pressure of 170 to 200 MN m^{-2}, which were then sintered at high temperature. Details of firing and sintering procedures are given elsewhere [30]. After sintering, the two end surfaces were ground flat with a precision lapping device [31] to about ±1.5 μm. The flat faces were then polished. Densities of these pellets were between 70% and 82% of theoretical, as calculated from a knowledge of cell parameters and formula weights of the cubic unit cell. Denser discs (92% to 93% of theoretical density) of composition $(U_{0.7}Y_{0.3})O_{2+x}$ were prepared when required by calcining the co-precipitated hydroxides in argon or hydrogen at 800° C for 15 h, and then sintering cold-pressed pellets (170 to 200 MN m^{-2}) of the resulting powder at 1500° C in an argon atomosphere for 100 h.

Kanthal Al resistance furnaces were used for the experiments. The constant temperature zone was approximately 6 cm in length (± 1° C); the length of the cell never exceeded 1 cm. 13% Rh–Pt/Pt thermocouples were used for temperature control and measurement. A diagram of the final version of the apparatus used in various experiments is shown in Fig. 1a.

2.2. Conductivity experiments

Platinum forms a strong bond to most ceramics when it is placed in firm contact with them at elevated temperatures (1000 to 1300° C) [32]. This property was used to attach annular Pt electrodes to both flat faces of the pellets for conductivity measurements: platinum lead wires were subsequently spot-welded to them. In some cases platinum paste (N758 Johnson Matthey Metals Ltd) was used between the platinum foil and the ceramic, especially for low density discs. Standard two-probe (a.c.) and four-probe (a.c. and d.c.) methods were used for electrical conductivity measurements. The two annular platinum electrodes sealed to the ceramic pellet were used as current leads (Fig. 1b). The potential probes were constructed from two platinum lead wires contained in a twin-bore alumina thermocouple sheath. These two wires were fused into a spherical bead at one end, and this was pulled tight against the end of the alumina sheath. In this way pressure could be applied to the probe-specimen contact via the rigid alumina component. Two such probes were positioned in the middle of the annular platinum electrodes and in contact with the specimen on both sides. Good contacts were maintained by applying light pressure to these probes. Since no current was permitted to flow through these probes, relatively high contact resistances could be tolerated. The potential used to supply current varied between 0.01 and 10 V for both four-probe d.c. and a.c. measurements: in most cases it was below 1 V and potential differences were measured with a digital voltmeter. Care was taken to avoid instability due to stray voltages. For two-probe a.c. measurement (1 kHz and 5 kHz) only the annular electrodes were utilized. The conductivity bridge used in these measurement was based on a design by Janz and McIntyre [33]. Measurements on most specimens were made in air but some measurements were also made in H_2, O_2, argon ($p_{O_2} = 3 \times 10^{-6}$ atm) and CO/CO_2 mixtures. Current distribution in the specimen as assembled for measurement was obtained by an analogue method [34, 35].

2.3. Electrodiffusion

The cell arrangement used for electrodiffusion experiment is shown in Fig. 2a. A constant current of 100 mA from a Keithley constant current source "Model 225" was passed continuously through the cell at 957° C for 384 h. The potential drop across the cell was monitored with two potential probes similar to those described previously. The experiment was done in air.

After completion of the experiment, all three pellets (both electrodes and the electrolyte) were cross-sectioned, mounted in epoxy resin, and polished. The specimens were studied optically with a Carl Zeiss optical microscope model

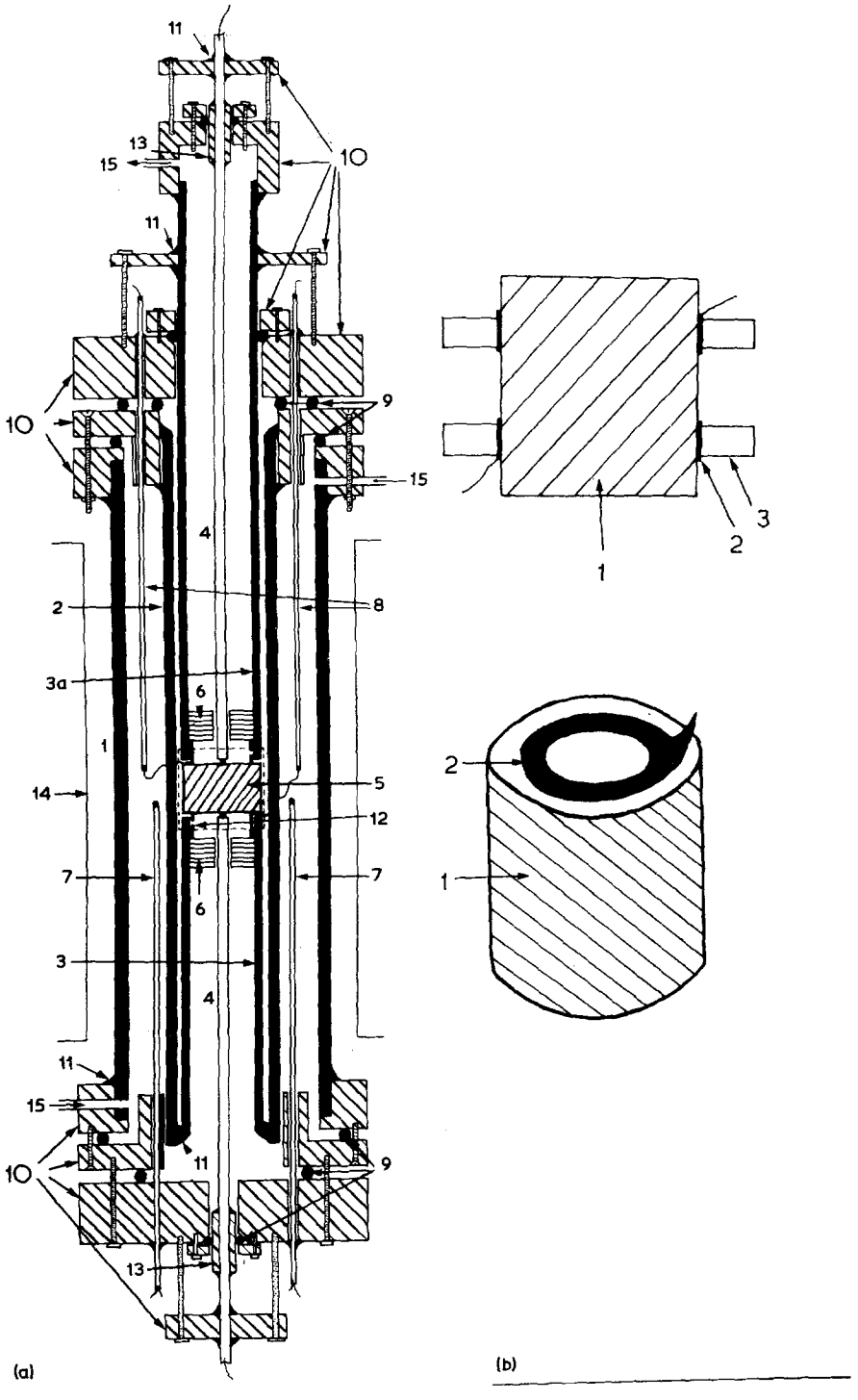

Figure 1 (a) Gas tight apparatus (horizontal). (1) Outer alumina tube with brass fittings glued at the ends. (2) Inner alumina tube with a slit in the middle. (3) Alumina tube (to support the cell components) glued to inner alumina tube (2) on one end. (3a) Alumina tube to support and apply pressure to cell components. (4) Platinum probes. (5) Cell components. (6) Pyrophlite pieces with 4.5 mm hole in the middle and glued to alumina tubes (3) with cerama bond 503. (7) Thermocouples. (8) Alumina sheathing for lead wires. (9) O-ring. (10) Brass fittings. (11) Epoxy resin. (12) Alumina rings with a small slit. (13) Stainless steel pieces. (14) Furnace. (15) Gas inlets and outlets.

(b) Sample with annular electrodes: (1) sample, (2) annular platinum electrodes, (3) alumina rings.

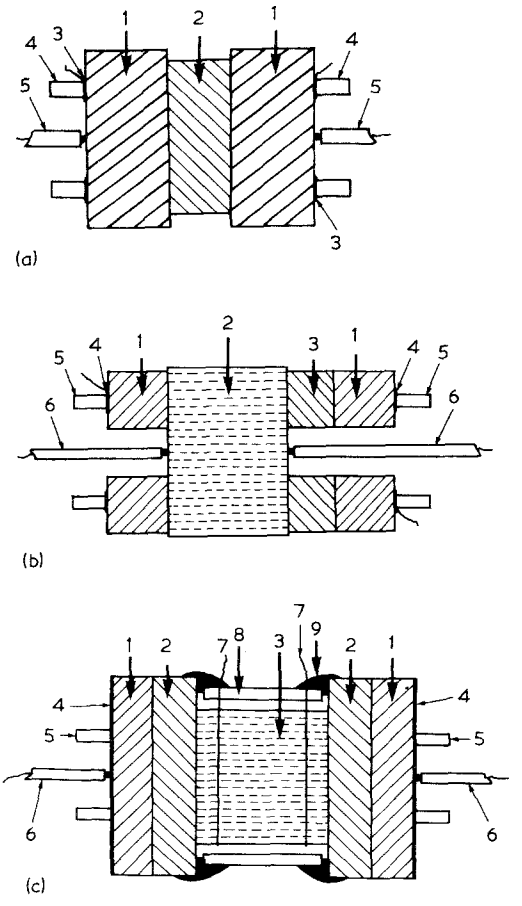

Figure 2 (a) (1) $(U_{0.7}Y_{0.3})O_{2+x}$ electrodes. (2) YSZ electrolyte disc. (3) Annular platinum contacts to the electrodes (1). (4) Alumina rings. (5) Platinum potential probes.

(b) (1) Cu/Cu_2O pellets. (2) Ceria sample. (3) YSZ electron blocking electrode. (4) Annular platinum contacts. (5) Annular alumina rings to support the cell components. (6) Platinum potential probes.

(c) (1) Cu/Cu_2O discs. (2) YSZ electron blocking electrodes. (3) $(U_{0.7}Y_{0.3})O_{2+x}$ sample. (4) Platinum foil. (5) Alumina rings to support the cell components. (6) Platinum contacts to platinum foil. (7) Platinum potential probes. (8) Alumina guard tube. (9) Glass seal.

"Ultraphot III B". Electron microprobe analyses were carried out with a "JXA-3A Electron Probe X-Ray Microanalyser", capable of analysing two elements simultaneously.

2.4. Transport number determination

Attempts to measure ionic transport numbers were made using a simple blocking electrode technique [36, 37]. The assembly used initially is shown in Fig. 2b. Experiments were first carried out with ceria (Spec pure: Johnson Matthey) to test the method since data for ceria are extant [38–45], and the results obtained were encouraging. Accordingly experiments were then made with this assembly on urania–yttria solid solutions. Many of these were unsuccessful due to stray Faradaic processes which resulted from gas-phase effects at the specimen–blocking electrode interfaces. Finally, this problem was overcome to a large extent by isolating these interfaces from contact with the gas phase. The assembly incorporating this modification is shown in Fig. 2c.

The electron-blocking electrodes used were 90 mol% ZrO_2 – 10 mol% Y_2O_3. Cu/Cu_2O pellets in contact with these, on the side away from the specimen $[(U_{0.7}Y_{0.3})O_{2+x}]$ pellets (density 93% of theoretical) were used as source and sink for oxygen transported. All experiments were carried out in a stream of purified argon, and a four-probe method for conductivity measurement was used. The currents used were less than 30 μA, and the potential drop across the probe electrodes was measured with a chart recorder. When these experiments were completed the blocking electrodes were replaced by platinum foil and the *total* electrical conductivity of the specimen measured.

3. Results and discussion

3.1. Conductivity experiments

Measurements on all samples were made during several heating and cooling cylces until reproducible results were obtained, indicating that the whole assembly of electrodes and polycrystalline sample had stabilized. Data for the last heating and cooling cylces were considered to be more reliable and are reported. The results show no significant difference between the four-probe a.c. and four-probe d.c. values of resistance at all temperatures. By contrast, however, two-probe a.c. values for the resistance were 3 to 6 times higher as compared to the corresponding data obtained from four-probe measurements, which indicates a considerable contact resistance at the annular platinum electrode–specimen interface. Since these measurements were only carried out to explore the potential of various materials as solid oxide electrodes, precise data on specific conductivities were not required and so the results presented are resistances for the various samples as measured, and are also not corrected for porosity.

However, specific resistances (ρ_s) can be calculated [46, 47] for the type of probe arrangement used, knowing the ratio of probe spacing to

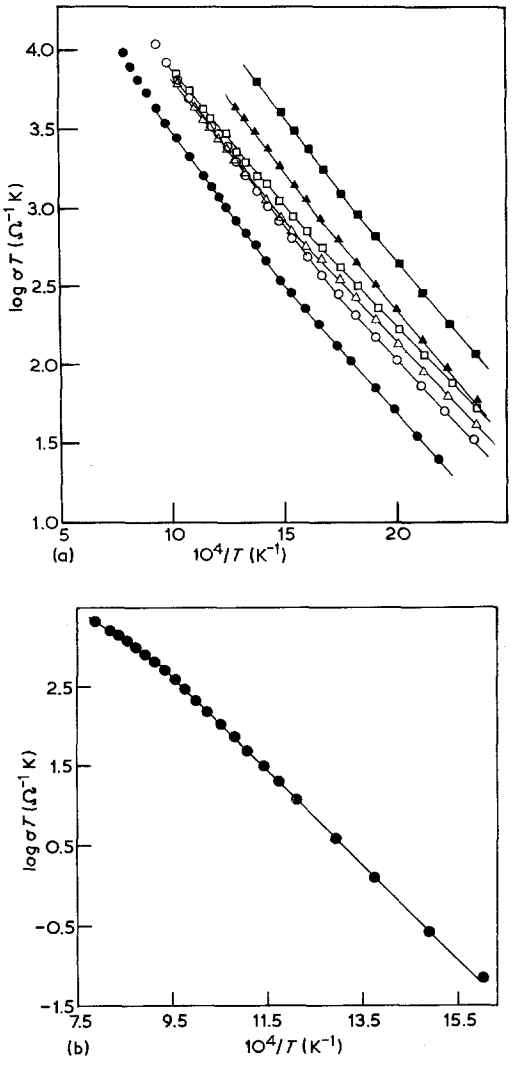

Figure 3 Plots of $\log \sigma T$ versus $10^4/T$ for various samples: (a) ■ $(U_{0.7}Y_{0.3})O_{2+x}$, ▲ $(U_{0.6}Y_{0.4})O_{2+x}$, ○ $(U_{0.5}Y_{0.5})O_{2+x}$, □ $(U_{0.45}Y_{0.55})O_{2+x}$, △ $(U_{0.4}Y_{0.6})O_{2+x}$, ● $(U_{0.35}Y_{0.65})O_{+x}$. (b) ● $(U_{0.3}Y_{0.7})O_{2-x}$.

thickness for each pellet and using the relation

$$\rho_s = 2\pi sR \times \text{C.F.} \qquad (1)$$

where s is probe spacing, C.F. is a correction factor which is a function of the probe spacing to thickness ratio, and R is the measured resistance. The thicknesses of the pellets were within 4 to 6 mm and the spacing between potential and current probes varied between 2.5 to 3.5 mm. Calculations based on the above equation show that in order to get specific resistance, the measured resistance has to be multiplied by a factor of 2.5 to 4.0 for most of the pellets. However, information obtained from the analogue simulation of a two-dimensional model of the electrode arrangement suggests a factor of 3.2 as compared to 2.5 calculated for the same probe spacing to thickness ratio using the first method.

Measurements on most of the samples were carried out between room temperature and 700 to 800° C, but in cases where the resistance of the samples was still high enough to be measured, measurements were made up to 1000° C. Log σT versus $1/T$ plots for one representative heating or cooling cycle in air for each sample are given in Figs. 3a and b. These plots are well described by two straight lines of slightly different slopes, intersecting at about 350° C. The slight curvature of points from the line at the highest temperature is probably due to small composition changes in the sample. Such effects were observed much more dramatically on samples which had been prepared in air and then measured in hydrogen. Figs. 3a and b show that the $(U_{0.7}Y_{0.3})O_{2+x}$ composition has the highest conductivity in air, and it was for this reason that other types of experiments (electrodiffusion, transport number determination) were carried on samples of this composition.

The results from a $(U_{0.7}Y_{0.3})O_{2+x}$ sample prepared in an argon atmosphere (density of the pellet 92% to 93% of theoretical) and measured in argon, CO/CO_2 (1:1.4), O_2 and air are shown in Fig. 4. The activation energy of this sample was slightly higher than that of the less dense disc of

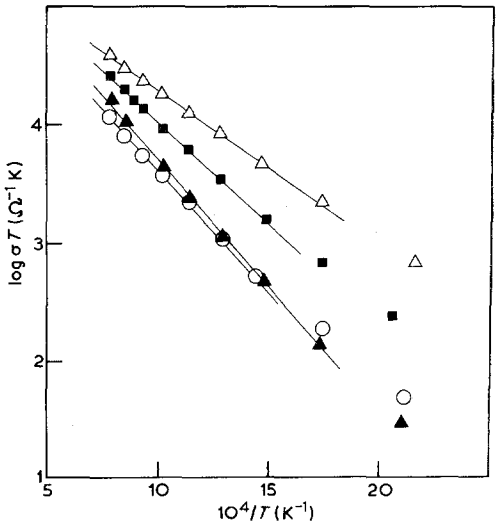

Figure 4 Plots of $\log \sigma T$ versus $10^4/T$ for $(U_{0.7}Y_{0.3})O_{2\pm x}$ in various gas atmospheres: ○ oxygen (1 atm), △ air (0.28 atm), ■ argon (3×10^{-6} atm), ▲ CO/CO_2 (1:1.4). Sample prepared in argon, density 92% to 93% of theoretical, correction factor (see text) = 1.5.

TABLE II Energies of activation (E) for the conductivity of urania–yttria (scandia) fluorite-type solid solutions

Sample*	E‡ (kJ mol^{-1})	
	Low-temperature region (below ~ 350° C)	High-temperature region (above ~ 350° C)
$(U_{0.7}Y_{0.3})O_{2+x}$	32.4 ± 1.0	36.2 ± 1.5
$(U_{0.6}Y_{0.4})O_{2+x}$	32.6 ± 0.6	33.7 ± 1.5
$(U_{0.5}Y_{0.5})O_{2+x}$	29.4 ± 0.8	38.7 ± 1.7
$(U_{0.45}Y_{0.55})O_{2+x}$	28.2 ± 0.5	32.8 ± 0.8
$(U_{0.4}Y_{0.6})O_{2+x}$	29.1 ± 0.6	35.4 ± 0.4
$(U_{0.35}Y_{0.65})O_{2+x}$	31.1 ± 0.4	37.6 ± 0.6
$(U_{0.3}Y_{0.7})O_{2-x}$	–	114.4 ± 1.4 (83.1 ± 4.0)†
$(U_{0.5}Sc_{0.5})O_{2+x}$	19.3 ± 0.5	21.7 ± 0.5
$(U_{0.38}Sc_{0.62})O_{2+x}$	14.0 ± 0.4	15.8 ± 0.4
$(U_{0.7}Y_{0.3})O_{2+x}$ (oxygen)	–	39.6 ± 2.4
$(U_{0.7}Y_{0.3})O_{2+x}$ (air)	–	41.8 ± 1.3
$(U_{0.7}Y_{0.3})O_{2+x}$ (argon)	–	33.0 ± 1.2
$(U_{0.7}Y_{0.3})O_{2+x}$ (CO/CO_2)	–	24.8 ± 0.7

*Conductivity measurements were done in air unless otherwise specified.
†Figures in parentheses are for temperature between 850 and 1000° C.
‡Activation energies were calculated for several heating and cooling cycles and 2 to 3 samples were measured for most of the compositions.

same composition. Activation energies (obtained from log σT versus $1/T$ plots) for conductivity in various samples under different conditions for both temperature regions are given in Table II. These were 20% to 30% higher than those obtained from log R versus $1/T$ plots. The low energy of activation for conductivity below 350° C is probably associated with impurity-controlled, history-dependent processes.

Hund *et al.* [24] also studied three compositions in the fluorite-type urania–yttria solid solution region. For one common composition, namely $(U_{0.6}Y_{0.4})O_{2+x}$, the activation energy (32.6 kJ mol^{-1}) determined by them is in fair agreement with the value (33.7 kJ mol^{-1}) obtained in this work.

As with UO_{2+x} [48–50], urania–yttria solid solutions are hopping-type semi-conductors. In this work O/M ratios under varying conditions have not been determined, but an estimate of these can be obtained from data extant for the systems urania–neodymia [51] and urania–lanthana [52].

In air, Aitken [53] has shown that the O/M ratio for $(U_{0.45}Y_{0.55})O_{2+x}$ and $(U_{0.40}Y_{0.60})O_{2+x}$ is close to 2.0 at 1300° C. For $(U_{0.50}Nd_{0.50})O_{2+x}$ in air at 850° C, this ratio is also close to 2.0, and similar results were reported by Diehl and Keller [54] for the urania–lanthana system. Thus the O/M ratio in air can be assumed almost to be constant at 2.0 over a wide range of U/Y ratios (0.35/0.65 to 0.50/0.50). For $(U_{0.7}Y_{0.3})O_{2+x}$, however the O/M ratio in air is about 2.21 at ~780° C and about 2.18 at 1000° C [30]. It is to be noted that the conductivity of $(U_{0.7}Y_{0.3})O_{2+x}$ in air is significantly higher than that of other samples, but in a CO/CO_2 atmosphere (1/1.4) it is, surprisingly, higher than in air and the activation energy (24.8 kJ mol^{-1}) is lower. Further reference to the French thermodynamic work on urania–neodymia shows that under these conditions the O/M ratio is now less than 2.0. Thus, conductivity and activation energy depend in a complex fashion on both the U/Y and O/M ratios. The $(U_{0.3}Y_{0.7})O_{2-x}$ sample had a very high resistance and no data could be recorded below 300° C. However, the Arrhenius plot for this sample changed slope around 850° C indicating a different activation energy (see Fig. 3b). It was yellow in colour as compared to a greenish brown or greenish black colour for the other compositions, suggesting that the uranium was completely oxidized to U^{6+}: the O/M ratio then calculates as 1.95. Moreover, the high energy of activation observed between 300 and 850° C lies in the region for oxygen ion conduction. This, however, is less significant criterion and no definite conclusions can be drawn from this quantity alone. Further experiments need to be carried out to check this possibility, but if the conduction is predominantly ionic the data show that this material is a significantly better conductor than

YSZ (8 to 10 times) and CeO_2–Gd_2O_3 (2 to 3 times) [55]. Above $\simeq 850^\circ$ C, however, the slope of the Arrhenius plot decreases markedly ($E \simeq 83\,kJ\,mol^{-1}$), which probably represents the onset of n-type electronic conduction.

3.2. Electrodiffusion

No uranium in excess of 0.3 wt% (the detection limit of the instrument) was detected in the ZrO_2–10 mol% Y_2O_3 electrolyte disc: the cut-off at the interfaces between the electrode and electrolyte pellet was very sharp. Moreover, the zirconium and yttrium concentrations were uniform throughout in the electrolyte disc. Likewise for both the cathode and anode electrode discs of $(U_{0.7}Y_{0.3})O_{2+x}$ uniform concentrations of uranium and yttrium were observed.

Uranium self-diffusion coefficients are very low in UO_{2+x} [56–58] and similar cation diffusion coefficients could be expected in urania-yttria fluorite-type solid solutions. Thus the results obtained, which indicated virtually no electrodiffusion of cations from electrode into electrolyte and vice versa over the period of current passage, are not surprising having regard to the time scale of the experiment (384 h) and the limited resolution (2 μm) of the electron probe.

Optical micrographs of the cathode electrode disc indicated a more porous structure (compared with the bulk) where this disc was in contact with the electrolyte pellet. However, the anode electrode pellet seemed to have uniform pore distribution (Fig. 5). This was further confirmed in scanning electron micrographs (Fig. 6).

The higher porosity of the cathode pellet close to the electrode–electrolyte interface (150 to 200 μm in extant) may prove to be disadvantageous in a practical situation since cracking can be seen clearly in this region at low magnification (Fig. 6). The cause of this is probably enhanced sintering of the polycrystalline material in the prevailing reducing conditions: it is well known [59] that urania samples sinter much better in reducing atmospheres, and this same effect has been observed here (see Section 2.1 above) for urania–yttria samples.

3.3. Transport number determination

In all the experiments except the last, where a symmetrical cell arrangement (i.e. two blocking electrodes) was used, the direction of the O^{2-} ion current was left to right, i.e. the side of the blocking electrode (YSZ) in contact with the specimen was the negative side. The reasons for choosing this direction for current flow were the following.

If the side of the specimen in contact with YSZ is anodic (positive), oxygen evolution can occur at the electrode–electrolyte interface. Urania–yttria or ceria, being good electronic acceptors, the reaction O^{2-} (YSZ) $\rightarrow \frac{1}{2}O_2 + 2e$ can occur at this

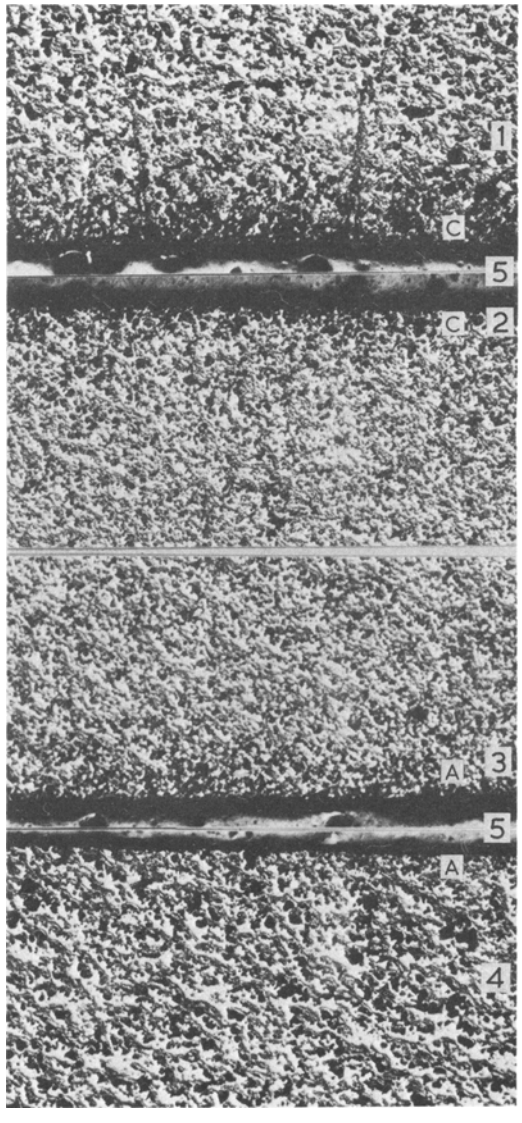

Figure 5 Optical photomicrographs of $(U_{0.7}Y_{0.3})O_{2+x}$/YSZ interfaces after passage of current, C cathodic interface, A anodic interface. (1) Cathode disc. (2) Cathode side of the electrolyte disc. (3) Anode side of the electrolyte disc. (4) Anode (5) Epoxy resin. (magnification × 40)

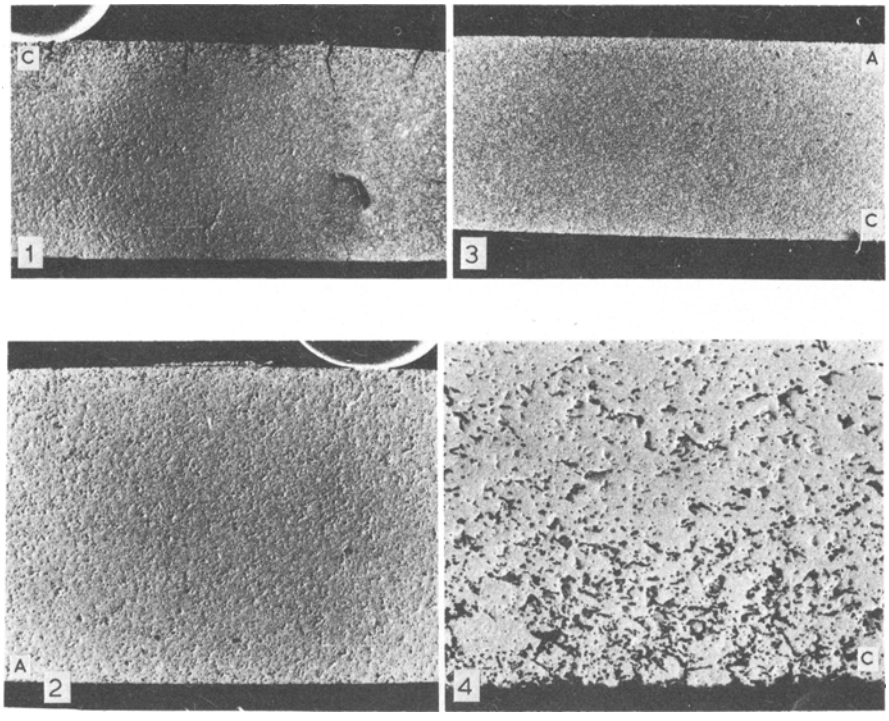

Figure 6 Scanning electron photomicrographs of $(U_{0.7}Y_{0.3})O_{2+x}$ electrodes and YSZ electrolyte discs, C cathodic interface, A anodic interface. (1) Cathode disc. (2) Anode disc. (3) Electrolyte disc. Magnification X 23.5. (4) Cathode disc. (X 145)

interface, permitting an electron current to flow in the specimen. Hence the platinum probes in contact with the sample will measure a potential drop corresponding to total conductivity. On the other hand if the side of the specimen in contact with YSZ is cathodic (negative), the reduction of oxygen, according to the reaction $\frac{1}{2}O_2 + 2e \rightarrow O^{2-}$, will be minimized once the concentration of oxygen in the gas phase is low. Thus electrons will be blocked but O^{2-} ions can pass through the blocking electrode (YSZ). However, one important point must be taken into account, i.e. if the oxygen reduction reaction is occurring to some extent in these experiments, then the measured oxygen ion transport numbers (t_i) will be higher than the true ones.

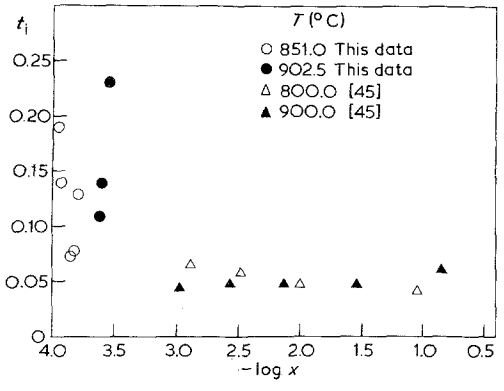

Figure 7 A plot of t_i versus $-\log x$ for CeO_{2-x}.

The results of transport number determination for CeO_{2-x} (Fig. 2b) as a function of $-\log x$ are shown in Fig. 7 and compared with the literature [45]: the agreement is fair.

For the $(U_{0.7}Y_{0.3})O_{2+x}$ sample (Fig. 2c), initially, i.e. before the glass seal became effective, the measured resistance was low and no transients were observed on switching the current, but as the temperature was increased to $\simeq 800°$ C or above and the glass seal melted, transient effects on switching were observed; the probe voltage rose suddenly to a maximum and then decayed to an almost constant value over a period of time (10 to 15 min). Similar transient behaviour was found on switching off the current (Fig. 8). Resistance was calculated from the steady state value of the probe voltage at constant current.

Ionic transport numbers were calculated from these data and are given in Table III. Measurements were made at three different temperatures, both with and without blocking electrodes.

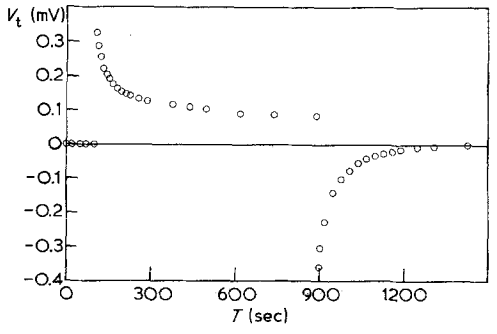

Figure 8 Transient behaviour of platinum probes for $(U_{0.7}Y_{0.3})O_{2+x}$ sample at 799° C, $I = 10\,\mu A$.

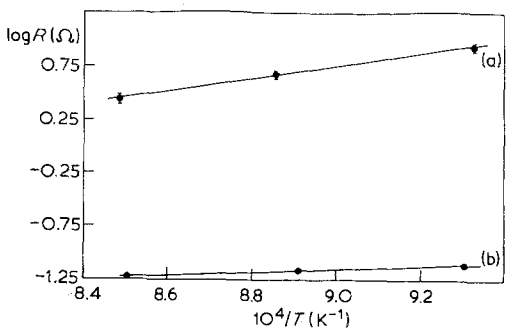

Figure 9 Arrhenius plot for the (a) ionic resistance (b) total resistance of $(U_{0.7}Y_{0.3})O_{2+x}$ sample.

The plots of $\log R$(ionic) versus $1/T$ (a) and $\log R$(total) versus $1/T$ (b) are given in Fig. 9; the energy of activation for ionic conduction was $110.9 \pm 8.4\,kJ\,mol^{-1}$, which lies well in the region for oxygen ion conduction in the fluorite-type oxides, while that claculated for total conduction was $27.2 \pm 2.1\,kJ\,mol^{-1}$, close to the value ($25.9 \pm 2.1\,kJ\,mol^{-1}$) obtained in the total conductivity measurements on a similar sample in argon from $\log R$ versus $1/T$ plots.

From the value of ionic conductivity at each temperature the specific conductivity (σ_i) was calculated. From the urania–neodymia data [51] it is known that the O/M ratio at an oxygen partial pressure of about 10^{-8} atm is $\simeq 2.012$. Diffusion coefficients (D) for oxygen ions in urania-yttria were calculated (Table III) using the Nernst–Einstein equation and assuming this composition

$$\sigma_i = \frac{DN(ne)^2}{kT} \qquad (2)$$

and

$$D_T = f \times D \qquad (3)$$

where $n = 2$ for O^{2-}, e is the charge of an electron, k is the Boltzman constant, T is the temperature in K, N is the total number of charge carriers (O^{2-}) per cubic centimetre in the U_3O_8–Y_2O_3 lattice, and D_T the tracer diffusion coefficient. A value of 0.65 for the correlation factor f was used [60, 61], although the mechanism of anion diffusion in urania–yttria is not known. The values of D_T listed in Table III are about two orders of magnitude greater than those determined directly from ^{18}O tracer studies [62]. This discrepancy is discussed below.

3.4. Analysis of transients

Transient behaviour on switching, similar to that described above, has been interpreted by Roth and Ramanczuk [63] in terms of an equivalent circuit consisting of electronic and ionic resistors in parallel and a capacitor in series with the ionic resistor. The capacitor represent the effects of the ion blocking electrode in his work. In a case where two sets of voltage probes (one reversible to ionic carriers and the other to electronic carriers) are used, the switching of a constant current through this circuit leads to complementary exponential rises and decays in the e.m.f.s of both types of voltage probes characterized by a time constant given by [37]

$$\tau = (R_e + R_i)C \qquad (4)$$

TABLE III Results of ionic conductivity, transport numbers and diffusion coefficents for $(U_{0.7}Y_{0.3})O_{2+x}$

Temperature (° C)	R_i* (Ω)	R_T (Ω)	t_i	Specific† conductivity ($\Omega^{-1}\,cm^{-1}$)	$D \times 10^{11}$ ($m^2\,sec^{-1}$)	$D_T \times 10^{11}$ ($m^2\,sec^{-1}$)
799.0	8.5 ± 0.5		0.0092	0.053	1.4	0.9
802.0		0.078				
856.0	4.75 ± 0.25		0.0143	0.096	2.7	1.8
849.0		0.068				
905.4	2.75 ± 0.25		0.0218	0.165	4.9	3.2
902.5		0.060				

*Results reproducible within a factor of 1.5 on cooling.
†Specific resistance = $R_i \times 2.2$.

where

$$C = \frac{AZ}{\pi^2} \frac{F\rho}{M\,\mathrm{d}E/\mathrm{d}x}. \quad (5)$$

Also

$$\frac{1}{\tau} = \frac{\bar{D}\pi^2}{Z^2} = \frac{\pi^2}{Z^2} \frac{\sigma_i \sigma_e}{\sigma_i + \sigma_e} \frac{M}{F\rho} \frac{\mathrm{d}E}{\mathrm{d}x}, \quad (6)$$

where $\bar{D}$ is the chemical diffusion coefficient, M the molecular weight, ρ the density of the material Z the length of the sample, A the area of cross section of specimen, F the Faraday constant, and $\mathrm{d}E/\mathrm{d}x$ the electrochemical potential gradient.

Dudley and Steele [37] used two sets of probes and passed both electronic and ionic currents seperately through potassium ferrite, measuring the responses of each set of probes for each type of current. In both cases the voltage across probes reversible to the blocked carriers returned closely to the value obtaining before current was passed.

The data obtained on urania–yttria were more complicated because only one set of probes (platinum) was used. These are reversible both to ionic and electronic current carriers. The observed response, when compared with the results of Steele and Dudley, clearly indicated a dual response by the platinum probes. Thus the steady state voltage may not be the true ionic IR drop, since there will be some compromise determined by the relative values of the ionic and electronic exchange currents. However, an analysis of the urania–yttria data similar to that of Dudley and Steele was carried out since in their work, the time constant for the exponential rise and decay of the e.m.f.s for each set of probes was the same. The time constant τ was calculated from the slope of plots of $\log(V_t - V_\infty)$ versus time, neglecting short times. V_∞ is the steady state voltage corresponding to the given current and V_t is the voltage at time t. $\bar{D}$ values calculated from the transients observed (see Equation 6) are given in Table IV. These values agreed to within ±10% for different currents.

Furthermore, since the ionic transport numbers are small in urania–yttria the term, $\sigma_e/(\sigma_i + \sigma_e) \simeq 1$ in Equation 6.

Thus

$$\bar{D} = \frac{\sigma_i M}{F\rho} \frac{\mathrm{d}E}{\mathrm{d}x}. \quad (7)$$

$\bar{D}$ values can also be calculated from this relation by inserting the measured σ_i values (Table III), and an estimate of $\mathrm{d}E/\mathrm{d}x$. The order of magnitude of $\mathrm{d}E/\mathrm{d}x$ was obtained from neodymia thermodynamic data [51] at 850° C near 10^{-8} atm oxygen partial pressure. $\bar{D}$ values thus determined are shown in Table IV.

An approximate energy of activation was calculated for chemical diffusion coefficients obtained from τ values: this was 92.0 ± 25.1 kJ mol^{-1} as compared with 110.9 ± 8.4 kJ mol^{-1} obtained from ionic conductivity data. If it can be assumed that $\mathrm{d}E/\mathrm{d}x$ is not strongly temperature dependent, these two activation energies should be similar.

The chemical diffusion coefficients given in Table IV are very high. However, the error in all these measurements is considerable as the voltages measured were less than 1 mV. Thus only orders of magnitude can be stated.

In attempting to assess the validity of the experimental results on ionic transport numbers two disturbing features stand out. First, the two orders of magnitude difference between calculated and observed D_T values, and secondly the very high $\bar{D}$ values which derive from analysis of transient behaviour. As indicated previously, it is extremely difficult to completely block Faradaic reaction at the urania–yttria/YSZ interface. A small fraction of the current can then be electronic as a result of the process $O_2 + 4e \rightarrow 2O^{2-}$ at this interface, for which the exchange current density is in any case high [26]. Moreover, the activation energy for charge transfer reaction across urania–yttria/YSZ interface is around 167 kJ mol^{-1}, and this could effectively determine the high apparent activation energy for the measured conductivity, which might otherwise be interpreted as associated with ionic transport. This situation will then correspond to the partially blocking case. It can never be guaranteed that leakage of oxygen through the glass seal is completely avoided. Indeed, there was

TABLE IV Chemical diffusion coefficients

Temperature (° C)	$\bar{D}_T$* × 10^8 ($\mathrm{m^2\ sec^{-1}}$)	$\bar{D}_T$† × 10^8 ($\mathrm{m^2\ sec^{-1}}$)
799.0	4.1 ± 0.4	2.1
856.0	8.1 ± 0.9	3.8
905.4	10.5 ± 1.5	6.6

*Chemical diffusion coefficients calculated from transients.

†Chemical diffusion coefficients calculated from σ_i (obtained from steady state probe voltage).

some indication of this: during an experiment in which the glass seal broke, the resistance dropped by a factor of two.

Calculations for the data show that even if more than 99% of the total electronic current was blocked, the remaining $<1\%$ contribution will increase the total conductivity measured at least by an order of magnitude.

On the other hand these attempts to measure ionic transport numbers in urania–yttria may have been more successful than appears from the above discussion. It is the discrepancy of two orders of magnitude between measured D_T values and those calculated from the conductivity data by means of the Nernst–Einstein equation which has led to the doubt expressed. However, there are considerable uncertainties about the application of this equation when the ionic transport number is extremely low, as it certainly is in this case. In this context it is worth noting that the values of D_T estimated by van Handel and Blumenthal [45], using the Nernst–Einstein equation, are also about two orders of magnitude higher than those measured directly by Steele and Floyd [64].

4. Conclusions

All available experimental evidence on urania–yttria solid solutions suggests that these materials are potential electrode materials for future use in high-temperature fuel and steam electrolysis cells. The fluorite-type phase exists over a wide composition range (30 to 70 mol% $YO_{1.5}$) in air and oxygen. Moreover, these materials are structurally stable in strongly reducing atmospheres such as CO or H_2. The conductivity in these fluorite-type solid solutions is mainly electronic. The $(U_{0.7}Y_{0.3})O_{2+x}$ composition had the maximum conductivity and is around two orders of magnitude higher than that of yttria-stabilized zirconia. Thus *IR* losses in the fuel cell will be mainly across YSZ. The conductivity is even higher in reducing atmospheres. This opens up the possibility that the same material can be used as anode and cathode. Overpotential losses at the $(U_{0.7}Y_{0.3})O_{2+x}$/YSZ interface are small [26] compared with Pt/YSZ interface. Virtually no interdiffusion of cations of the electrode or electrolyte material occurs under the working conditions of the cell because of their fixed positions in the fluorite sublattice. A thin layer of this electrode material painted on YSZ disc from its aqueous slurry and subsequently sintered in an argon atmosphere, adhered on to its surface and did not come off during several heating and cooling cycles. This indicates that urania–yttria solid solutions and YSZ have matching thermal expansion. These electrode materials are chemically inert with respect to the electrolyte at least up to 1300° C. Loss of weight for $(U_{0.7}Y_{0.3})O_{2+x}$ composition was observed in air and oxygen above 1400° C. However in an atmosphere no appreciable loss of weight was observed up to 1550° C. Other compositions studied were stable even above 1400° C in air or oxygen. Thus it seems that U_3O_8–Y_2O_3 fluorite-type solid solutions fulfil almost all the requirements of a high-temperature cathode or anode. Mainly technological problems remain to be solved.

Moreover, the $(U_{0.3}Y_{0.7})O_{2-x}$ composition may prove to be suitable electrolyte material. If the conductivity is truly ionic, it is 8 to 10 times higher than that of yttria-stabilized zirconia and this would have profound implications in many areas. More work is in progress to establish this.

Acknowledgement

We gratefully acknowledge many useful discussions with Dr. B. C. H. Steele.

References

1. T. H. ETSELL and S. N. FLENGAS, *J. Electrochem. Soc.* **118** (1971) 1890.
2. J. WEISBART and R. RUKA, *ibid.* **109** (1962) 723.
3. B. H. P. LTD. AUSTRALIA, CRL Reports on High-Temperature Fuel Cells (1969–72), Private communication.
4. F. J. ROHR, in "Solid Electrolytes", edited by P. Hagenmuller and W. van Gool (Academic Press, London, New York, 1978) p. 431.
5. "Proceedings of the Workshop on High Temperature Solid Oxide Fuel Cells", edited by H. S. Isaacs, S. Srinivasan and I. L. Harry (U.S. Dept. of Energy BNL 50756/TID-4500, 1977).
6. B. C. H. STEELE, "Electrode Processes in Solid State Ionics", edited by M. Kleitz and J. Dupuy (Reidel, Dordrecht, 1976) p. 367.
7. H. S. SPACIL and C. S. TEDMON Jr, *J. Electrochem. Soc.* **116** (1969) 1618, 1627.
8. H. S. SPACIL and K. W. BROWALL, *ibid.* **121**, (1974) Abstr. 231 (The Electrochemical Soc. Inc., New York Meeting, New York, 1974).
9. A. AYPAR, *Technical J.* 1 (1974) 137.
10. T. TAKAHASHI, in "Physics of Electrolytes", Vol. 2, edited by J. Hladik (Academic Press, London, New York, 1972) p. 989.
11. J. W. PATTERSON, *J. Electrochem. Soc.* **118** (1971) 1033.
12. H. TANNENBERGER, H. SCHACHNER and P. KOVACS, *Proc. J. Intl. Etude Piles Combust.* **1-III** (1965) 19.

13. J. W. PATTERSON, E. C. BOGREN and R. A. RAPP, *J. Electrochem. Soc.* **114** (1967) 752.
14. H. L. TULLER and A. S. NOWICK, *ibid.* **122** (1975) 255.
15. R. N. BLUMENTHAL, F. S. BRUGNER and J. E. GARNIER, *ibid.* **120** (1973) 1230.
16. T. KUDO and H. OBAYASHI, *ibid.* **122** (1975) 142.
17. R. M. DELL and A. HOOPER, in "Solid Electrolytes", edited by P. Hagenmuller and W. van Gool (Academic Press, London, New York, 1978) P. 291.
18. H. TANNENBERGER and H. SIEGERT, in "Fuel Cell Systems – II", Advances in Chemistry Series, Vol. 90 (American Chemical Society, Washington, D.C., 1969) 281.
19. O. ANTONSEN, W. BAUKAL and W. FISCHER, *The Brown Boveri Review* **53** (1966) 21.
20. D. W. WHITE, *Rev. Energ. Primaire* **2** (1966) 10.
21. C. S. TEDMON, Jr, H. S. SPACIL and S. P. MITOFF, *J. Electrochem. Soc.* **116** (1969) 1170.
22. D. D. BUTTON and D. H. ARCHER, Meeting of the *Amer. Ceram. Soc. Bull.* **45** (1966) 403.
23. T. H. ETSELL and S. N. FLENGAS, *Chem. Rev.* **70** (1970) 339.
24. VON F. HUND, U. PEETZ and G. KOTTENHAHN, *Z. Anorg. Allg. Chem.* **278** (1955) 184.
25. J. S. ANDERSON, I. F. FERGUSON and L. E. J. ROBERTS, *J. Inorg. Nucl. Chem.* **1** (1955) 340.
26. S. P. S. BADWAL, D. J. M. BEVAN and J.O'M. BOCKRIS, to be published.
27. E. SUMMERVILLE, Ph.D. Thesis, The Flinders University of South Australia (1973).
28. VON F. HUND and U. PEETZ, *Z. anorg. allg. Chem.* **271** (1952) 6.
29. W. TRZEBIATOWSKI and R. HORYN, *Bull. De L'Academie Palonaise Des Sciences* **XIII** (1975) 303.
30. S. P. S. BADWAL, Ph. D. Thesis, The Flinders University of S. A., Australia (1977).
31. H. J. DE BRUIN and R. L. CLARK, *Rev. Sci. Instrum* **35** (1964) 227.
32. H. J. DE BRUIN, A.F. MOODIE and C. E. WARBLE, *J. Mater. Sci.* 7 (1972) 909.
33. G. J. JANZ and J. D. E. McINTYRE, *J. Electrochem. Soc.* **108** (1961) 272.
34. B. H. S. DAY, *Metals Australia* **5** (1973) 34.
35. R. H. ROUSSELOT, *Metal finishing* **57** (1959) 56.
36. L. HEYNE, *N.B.S. (US) Spec. Publ. No. 296* (1967) 149.
37. G. J. DUDLEY and B. C. H. STEELE, *J. Solid State Chem.* **21** (1977) 1.
38. D. J. M. BEVAN and J. KORDIS, *J. Inorg. Nucl. Chem.* **26** (1964) 1509.
39. R. N. BLUMENTHAL and J. E. LAUBACH, "Anistropy in Single-Crystal Refractory Compounds", edited by W. Vahldiek and S. A. Mersol (Plenum Press, New York, 1968) p. 138.
40. R. N. BLUMENTHAL and R. J. PANLENER, *J. Phys. Chem. Solids* **31** (1970) 1190.
41. R. N. BLUMENTHAL, P. W. LEE and R. J. PANLENER, *J. Electrochem. Soc.* **118** (1971) 123.
42. R. N. BLUMENTHAL and R. L. HOFMAIER, *ibid.* **121** (1974) 126.
43. R. N. BLUMENTHAL, R. J. PANLENER and J. E. GARNIER, *J. Phys. Chem. Solids* **36** (1975) 1213.
44. R. N. BLUMENTHAL and R. K. SHARMA, *J. Solid State Chem.* **13** (1975) 360.
45. G. J. VAN HANDEL and R. N. BLUMENTHAL, *J. Electrochem. Soc.* **121** (1974) 1198.
46. P. A. SCHUMANN, Jr. and L. S. SHEINER, *Rev. Sci. Instrum.* **35** (1964) 959.
47. W. GEE and M. GREEN, *J. Phys. E.* **4** (1971) 70.
48. R. K. WILLARDSON and J. W. MOODY, "Uranium Dioxide", edited by S. Belle (USAEC, Washington, D.C., 1961) p. 243.
49. J. L. BATES, C. A. HINMAN and T. KAWADA, *J. Amer. Ceram. Soc.* **50** (1967) 652.
50. S. AMELINCKX *et al.*, "Physical Properties of UO_2 Single Crystals" (centre Etude Energie Nucl., Mol, EUR 1414. e, 1965).
51. J. F. WADIER, CAE-R4507 (Atomic Energy Commission, C.E.N., Fontenay-aux-Roses, France 1973).
52. E. STADLBAUER, U. WICHMANN, U. LOTT and C. KELLER, *J. Solid State Chem.* **10** (1974) 341.
53. E. A. AITKEN and R. A. JOSEPH, *J. Phys. Chem.* **70** (1966) 1090.
54. H. G. DIEHL and C. KELLER, *J. Solid State Chem.* **3** (1971) 621.
55. H. OBAYASHI and T. KUDO, in "Solid State Chemistry of Energy Conversion and Storage", Advances in Chemistry Series, Vol. 163, edited by J. B. Goodenough and M. S. Whittingham Chemical Society, Washington, D.C., 1977) p. 316.
56. A. B. LIDIARD, *J. Nucl. Mater.* **19** (1966) 106.
57. A. B. AUSKERN and J. BELLE, *ibid.* **3** (1961) 311.
58. S. YAJIMA, H. FURUYA and T. HIRAI, *ibid.* **20** (1966) 162.
59. J. R. JOHNSON and H. G. SOWMAN in "UO_2 Properties and Nuclear Applications", edited by J. Belle, (U.S. Atomic Energy Commission, Washington D.C. 1961) p. 321.
60. R. J. FERIAUF, in "Physics of Electrolytes", edited by J. Haldik (Academic Press, London 1972) p. 1103.
61. R. J. FERIAUF, *J. Appl. Phys.* **33** (1962) 494.
62. S. P. S. BADWAL and D. J. M. BEVAN, *Aust. J. Ceram. Soc.* **14** (1978) 1.
63. W. L. ROTH and R. J. RAMANCZUK, *J. Electrochem. Soc.* **116** (1969) 975.
64. B. C. H. STEELE and J. M. FLOYD, *Proc. Brit. Ceram. Soc.* **19** (1971) 55.

Received 28 November 1978 and accepted 28 March 1979.